

# Axially modified gallium phthalocyanines and naphthalocyanines for optical limiting

Yu Chen,<sup>\*abc</sup> Michael Hanack,<sup>b</sup> Yasuyuki Araki<sup>c</sup> and Osamu Ito<sup>c</sup>

Received 28th December 2004

First published as an Advance Article on the web 2nd March 2005

DOI: 10.1039/b416368k

Phthalocyanines (Pcs) offer a high architectural flexibility in structure, which facilitates the tailoring of their physical, optoelectronic and chemical parameters over a very broad range. This *tutorial review* describes the recent advances in the synthesis of soluble axially substituted or bridged gallium phthalo- and naphthalocyanine compounds, and their photophysical and nonlinear optical properties. The exploitation of the chemical reactivity of the Ga–Cl bond can allow the preparation of a series of highly soluble axially substituted and bridged Pc complexes. Axial substituents in Pcs influence favourably nonlinear optical absorption for the presence of a dipole moment perpendicular to the macrocycle in the axially substituted phthalocyanines. All Z-scans performed exhibit a decrease of transmittance about the focus typical of an induced positive nonlinear absorption of incident light. Substitution and dimerization of the phthalocyanine monomer resulted in significant reductions in the saturation energy density of the material displaying clear evidence of the usefulness of structurally modifying the gallium phthalocyanine unit. Similar to indium phthalocyanines, gallium phthalocyanines are also among the most promising materials that have been investigated as limiters of intense light and the current series presents a selection of structural modifications useful for varying their nonlinear optical properties.

\*chentangyu@yahoo.com



Yu Chen

Organic Chemistry, University of Tübingen, as Alexander von Humboldt research fellow (July 1, 2000–June 30, 2002) and as research associate (July 1, 2002–Oct. 30, 2002). At the end of Oct. 2002, he moved to the Department of Materials Science and Engineering, University of Washington at Seattle, USA, and worked with Prof. Alex K.-Y. Jen as research associate. In February 2004, he joined the Professor Osamu Ito's group at the Institute of Multidisciplinary Research for Advanced Materials, Tohoku University (Japan) as research scientist of CREST, JST. He has published 105 articles, of which more than 60 papers were published in international journals. His main research interests include organic synthesis; design and preparation of

Yu Chen, full professor of East China University of Science and Technology in Shanghai, was born in Sichuan, China in 1966. He received his PhD in Organic Chemistry under the direction of Prof. Dr. Zu-En Huang in July 1996. Since 1996 he has been a member of the Department of Chemistry at Fudan University where he spent 2 years earning his Associate Professor's position.

He joined Prof. Hanack's group at the Institute of



Michael Hanack

polymeric functional materials; fullerene chemistry; phthalocyanine chemistry; and photoinduced electron transfer processes of conjugated polymers.

Michael Hanack is Emeritus Professor of Chemistry at the University of Tübingen, Germany. He studied Chemistry in Freiburg, Bonn, and Tübingen, and received his PhD in Tübingen while working in the group of Walter Hückel on the kinetics and solvolysis of *p*-toluenesulfonates. He then "habilitated" in Tübingen in the area of organofluorine compounds and joined the University of the Saarland at Saarbruecken as a full Professor in 1971. In 1976 he returned to Tübingen, where he worked for several years in physical organic chemistry before moving into materials science around 20 years ago. His main interests are in the electrical and nonlinear optical properties of phthalocyanines and light-emitting polymers based on PPV-analogous materials. He has published more than 550 papers. Since 1964 more than 230 students have received PhD degrees in his group. For many years, he was one of the Editors of *Houben-Weyl*; currently he is a Regional Editor of *Synthetic Metals*.

## 1. Introduction

The highly delocalized aromatic 18  $\pi$ -electron system of phthalocyanines can give rise to a strong nonlinear optical (NLO) response. Similar to  $C_{60}$  and its organic and polymeric derivatives, phthalocyanines (Pcs) are materials that optically limit nanosecond light pulses over a fairly wide range of the UV/Vis spectrum *via* excited state absorption processes, and have been extensively investigated as being among the most promising of NLO materials due to their architectural flexibility, which allows tailoring of their physical, optoelectronic and chemical parameters in a broad range, having exceptional stability and processability features.<sup>1–4</sup> The nonlinear optical absorption mechanism of Pcs in the optical region comprised between Q- and B-bands involves the population of excited states which absorb more effectively than the ground state. This gives rise to the phenomenon of Reverse Saturable Absorption (RSA) as a consequence of multiphoton absorption.<sup>1,4</sup> It has been shown that phthalocyanine compounds exhibit RSA because of the occurrence of intersystem crossing from the lowest excited singlet state ( $S_1$ ) to the lowest triplet state ( $T_1$ ) and the subsequent increase in the population of the strongly absorbing  $T_1$  state with nanosecond dynamics.

The vast possibilities to chemically or physically modify Pcs allow tailoring the speed and magnitude of NLO responses to the target application. About 70 different elements have been incorporated into the phthalocyanine core. Many of the central metal elements have one or two sites which can coordinate to a variety of axial ligands. The introduction of a diversity of peripheral substituents and axial substituents, with many possibilities to alter the substitution pattern with respect to the number and position of the substituents, has a strong influence on the electronic absorption spectra and optical nonlinearities.<sup>5–7</sup> Other factors that affect optical nonlinearities are the length of  $\pi$ -electron conjugation, the crystal structure of the compounds, and the thin film fabrication techniques employed (if films can be made).<sup>1</sup> The third-order

NLO properties with phthalocyanines were first reported in 1987 for the peripherally unsubstituted chlorogallium phthalocyanine (PcGaCl) and fluoroaluminium phthalocyanine (PcAlF).<sup>8</sup> The  $\chi^{(3)}$  value for PcGaCl was half that of PcAlF at 1.064  $\mu\text{m}$ . After this, the  $\chi^{(3)}$  values of a various Pcs, including PcAlCl, PcInCl and PcTiO, were measured using THG techniques.<sup>1,9</sup> Comparison of  $\chi^{(3)}$  values of Pcs with and without axial ligands<sup>1</sup> indicates that Pcs with an axial ligand, for example PcVO, PcTiO, PcAlF, PcGaCl, PcInCl show a large  $\chi^{(3)}$  in THG experiments. Axial substitution in Pc complexes has provoked relevant changes on the electronic structure of the molecule by altering the  $\pi$ -electronic distribution due to the dipole moment of the central metal–axial ligand bond.<sup>7,10</sup> Studies of the NLO properties of Pcs have resulted in the identification of materials that are among the most promising optical limiting (OL) materials available. The optical limiting with Pcs was first reported for PcAlCl in 1989.<sup>11</sup> Experiments have been performed on many phthalocyanines *e.g.*  $R_n\text{PcM}$  ( $M = \text{Pb, Ni, Co, Cu, Zn, Si}; n = 4, 8$ ),  $M(\text{Pc})_2$  ( $M = \text{Eu, Gd, La}$ ),  $\text{SmH}(\text{Pc})_2$ ,  $t\text{Bu}_4\text{PcGe(OH)}_2$ ,  $\text{PcMX}$  with  $\text{MX} = \text{TiO, VO, InCl, GaCl}$ , and others in solution.<sup>1,3,4,7</sup> The best results obtained so far, however, concern soluble peripherally substituted indium phthalocyanines with an axial ligand.<sup>12</sup> The design and synthesis of new Pc-based optical active materials that simultaneously possess the physical, mechanical, and excellent NLO properties required for specific optical limiting applications is still a challenge for scientists. In this review we introduce the recent achievements on synthesis, photophysical properties and nonlinear optical (including optical limiting) properties of gallium phthalocyanines and naphthalocyanines.

## 2. Optical limiting response and optical limiters

Optical limiting is an important application of nonlinear optics, useful for the protection of human eyes, optical elements and optical sensors from intense laser pulses. An optical limiter is a device that strongly attenuates intense,



**Yasuyuki Araki**  
Yasuyuki Araki was born in 1970 in Japan and received his PhD degree from Tohoku University in 2000. He then joined Prof. Ito's laboratory as a postdoctoral fellow of CREST, JST. After 2 years he was promoted as research associate. His recent research interest is focused on the photoinduced electron transfer in the dyad or triad systems mimicking the photosynthetic reaction center containing [60]fullerene and building up photon-electron conversion devices by using these molecules.

**Osamu Ito**  
Osamu Ito was born in 1943 in Ibaraki, Japan, and received his PhD degree from the Graduate School of Science, Tohoku



**Osamu Ito**

University in 1973. He is currently a full professor of the Institute of Multidisciplinary Research for Advanced Materials of Tohoku University. His research interests mainly concern studies on the photochemistry reaction mechanism and photoinduced electron transfer processes of highly conjugated functional materials, *e.g.* fullerene derivatives, polyphenylenevinlenes, oligothiophenes, and others, by means of laser techniques in the wide wavelength and wide time regions. He has developed a selective scavenging flash photolysis technique that can be used to reveal the mechanism of reversible free radical reactions. He gained the 39th Mitsubishi Foundation Award in 2002.

potentially dangerous optical beams, while exhibiting high transmittance for low-intensity ambient light. As shown in Fig. 1, the optical limiting curve can be plotted as input fluence (or energy) vs. output fluence (or energy) (see upper panel in Fig. 1) or, input fluence (or energy) vs. transmittance (see lower panel). An important term in the optical limiting measurement is the limiting threshold. It is defined as the input fluence (or energy) at which the transmittance is 50% of the linear transmittance. It is obvious that the lower the optical limiting threshold, the better the optical limiting material. If different materials are measured with same linear transmission, the experimental and system errors can be minimized. Importantly, the error from the nonlinear scattering can be minimized too.

Several mechanisms giving rise to NLO responses can operate in a system. A perturbation of the electronic distribution in the material as a response to the electric field of the incident (low intensity) light is reason for normal linear polarization to occur. At high intensities, the electronic distribution no longer follows the applied field, resulting in both second- and third-order nonlinearities. The second common mechanism that can contribute to the NLO response is molecular reorientation. This mechanism can lead to nonlinear refractive indices with a picosecond response time but it will not contribute to the third harmonic generation signal. In general, an orientational nonlinearity can be larger than an electronic nonlinearity. Another important mechanism for a third-order NLO response is optical pumping. In this case the incident laser frequency approaches a transition

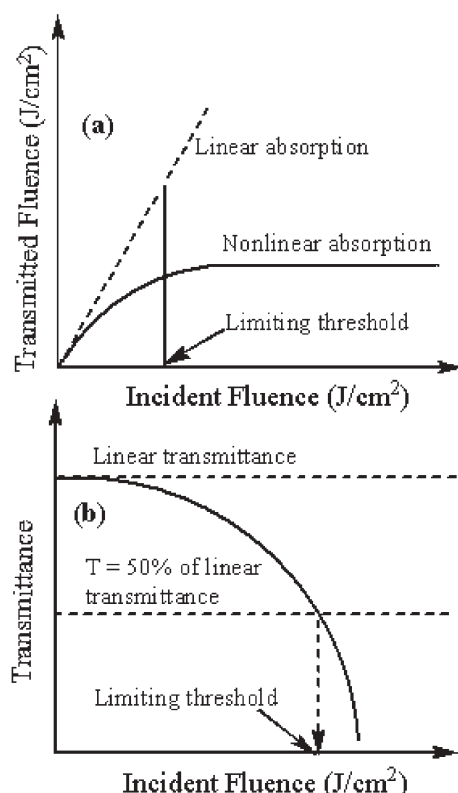


Fig. 1 The response of an optical limiter. An ideal limiter limits the output energy to some specified value.

frequency in the molecule. The light is absorbed causing transitions to an excited state. The optical properties of the excited state differ substantially from those of the ground state. The higher the population in the excited state is, the larger the changes in the optical properties of the material and the larger the optical nonlinearities are. Optical pumping involves real transitions to excited states. This is a big difference compared to the small perturbations of the electronic cloud mentioned above. This mechanism is the most important mechanism giving rise to saturable and reverse saturable absorption. Like the second mechanism, the response time for optical pumping is too slow to give rise to frequency mixing and harmonic generation but it does give useful nonlinear absorption and refraction. Fig. 2 gives a generalized five-level model used in calculation of excited state dynamics of the phthalocyanine system.<sup>13</sup> This mode describes the interaction of light with a molecular compound in terms of electronic transitions in the material. Within a few femtoseconds, the ground state ( $S_0$ ) of a molecule is excited to a higher vibronic level of the first singlet state ( $S_1$ ) by a laser with pulse width ( $\tau$ ). *Via* radiationless relaxation processes, the lowest vibronic level of  $S_1$  is reached within about a picosecond. Several competing processes can occur from here. These are further radiationless relaxation, fluorescence, or intersystem crossing from  $S_1$  to the triplet state ( $T_1$ ). The latter process sometimes takes place within several picoseconds. The very long lifetime of around many microseconds or longer of  $T_1$  reflects that the transition of  $T_1$  to  $S_0$ , known as phosphorescence, is forbidden by the selection rules for electronic transitions. The long lifetime of  $T_1$  is one of the prerequisites for a large positive nonlinear absorption coefficient.

Usually, the most important mechanism for optical limiting is nonlinear absorption and nonlinear refraction and nonlinear scattering as well. A negative nonlinear refractive index giving rise to self-defocusing of a light beam can cause substantial amounts of the energy of the incident light to be absorbed by

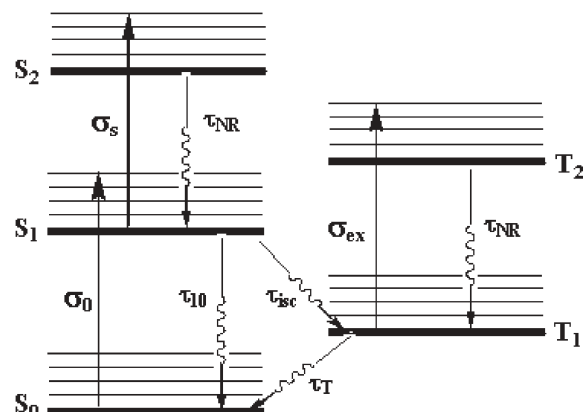


Fig. 2 Five level model diagram for phthalocyanines showing absorption (solid lines) and decay pathways (jagged lines).  $S_0$ ,  $S_1$  and  $S_2$  are singlet states;  $T_1$  and  $T_2$  are triplet states;  $\sigma_0$ ,  $\sigma_s$ ,  $\sigma_{ex}$ ,  $\tau_{NR}$ ,  $\tau_{10}$ ,  $\tau_{isc}$ ,  $\tau_T$  represent the ground state absorption cross-section, the first singlet excited state absorption cross-section, the first triplet excited state absorption cross-section, the nonradiative decay time, the first singlet excited state lifetime, the intersystem crossing time, the triplet excited state lifetime, respectively.

an exit aperture in the optical system. Materials with a positive nonlinear absorption coefficient exhibit reverse saturable absorption (RSA), and are characterized by a high transmission at normal light intensities and a decrease in transmission under high intensity or high fluence illumination. Conversely, the opposite situation, where the transmission increases with increasing incident intensity the process is termed saturable absorption (SA). The materials with SA usually have a negative nonlinear absorption coefficient. For optical limiters that rely on RSA from rapidly photogenerated transient states,<sup>14–16</sup> they are almost transparent for weak light but opaque for intense light. An efficient RSA material has a high ratio of excited state ( $T_1 \rightarrow T_2$ ) to ground state ( $S_0 \rightarrow S_1$ ) absorption cross section ( $\gg 1$ ), a rapid intersystem crossing rate ( $\tau_{isc} \ll \tau$ ), a long internal conversion lifetime, a high intersystem crossing quantum yield ( $\phi_{S_1 \rightarrow T_1} \sim 1$ ) and a long triplet lifetime ( $\tau_{T_1} \gg \tau$ ), the triplet state of the material absorbs the incoming laser so effectively that the laser can be greatly attenuated and the sensors can be protected. Two-photon absorption (TPA),<sup>17</sup> associated with the imaginary part of the third-order susceptibility, may also account for optical limiting. Basically in the visible region organic chromophore RSAs tend to have their primary absorption,  $\lambda_{max}(\pi-\pi^*)$ , at 400 nm, or below, to give reasonable transmission for solution or thin film measurements. Two-photon absorbers, on the other hand, would tend to depend on absorption in the 600–800 nm region to give rise to optical limiting effects in the visible.<sup>17</sup> TPA chromophores which limit between 600 and 800 nm via enhanced two-photon absorption would complement chromophores which limit between 400 and 600 nm by RSA. It would thus be very desirable if one could design OL chromophores that would function in a bimechanistic fashion: (1) RSA behavior at the high energy end of the visible, and (2) TPA behavior at the low energy end of the visible.<sup>17</sup>

In the case when the incident light is sufficiently intense so that a significant population accumulates in the excited state and if the material has an excited state absorption cross section  $\sigma_{ex}$  that is larger than the ground state cross section  $\sigma_0$ , the effective absorption coefficient of the material increases. To achieve the largest nonlinear absorption, both a large excited state absorption cross section and a long excited state lifetime are required. When the lifetime of the excited state being pumped is longer than the pulse width of the incident light, the changes in the absorbance and the refractive index are fluence ( $J \text{ cm}^{-2}$ ), not intensity ( $W \text{ cm}^{-2}$ ) dependent. Therefore, in materials with long upper state lifetimes, it is the fluence rather than the intensity that is limited. Limiting the fluence is usually desirable, since damage to optical devices is also often fluence dependent. Some criteria necessary for a large, positive nonlinear absorption are apparent including a large excited state cross section  $\sigma_{ex}$  and a large difference between the ground and excited state absorption cross sections ( $\sigma_{ex} - \sigma_0$ ). A variety of organic and organometallic materials, including porphyrins, metallophthalocyanines, fullerenes, organometallic cluster compounds and other materials have been found to fulfil these conditions.<sup>18–21</sup> For porphyrins and metallophthalocyanines, they can exhibit strong excited-state absorption, high triplet yields and long excited-state lifetime, while their

ground-state absorption is mostly confined to a few narrow regions (B and Q bands), allowing high transmission in the spectral window between these bands.<sup>1,21a</sup> The spectral bandwidth or window over which the limiter operates, and the ground-state and excited-state spectra and lifetimes, can be controlled or engineered by altering the axial or peripheral substituents, central metal cations and the structure of the main rings.

A practical optical limiter must operate over the wide range of incident intensities that might be encountered. The condition that  $\sigma_{ex}$  is greater than  $\sigma_0$  is necessary, but it is not sufficient for a useful OL material. The nonlinear response should possess a low threshold and remain large over a wide range of fluences before the nonlinearity saturates. A high saturation fluence normally requires a high concentration of the nonlinear material in the optical beam. For an organic material, this means it must be highly soluble in common organic solvents, or it is a pure liquid or a solid film that can be prepared with good optical quality. From the device point of view, the use of several successive limiters (tandem strategy) seems useful to optimize both the overall limiting and damage thresholds in phthalocyanines.<sup>4</sup> It should be noted that the response time of the nonlinear absorption and refraction in thin films of Pc materials may be strongly affected by intermolecular interactions.<sup>22</sup> The use of a heavy metal-Pc material together with an appropriate nonhomogeneous concentration profile along the beam path leads to greatly improved optical limiting devices.<sup>21a,23</sup>

### 3. Z-scan method for NLO studies

Most phthalocyanines are centrosymmetric materials except for monoaxially substituted Pc complexes like  $\text{PcTiO}$ ,  $\text{PcVO}$ ,  $\text{PcAlCl}$ ,  $\text{PcInCl}$  or  $\text{PcGaCl}$ . Third-order optical nonlinearities are therefore of main interest in Pc materials, as they can be large with sub-picosecond response times. The principal measurement techniques that have been used in NLO studies of Pcs are third harmonic generation (THG), degenerate four wave mixing (DFWM), electric field induced second harmonic generation (EFISHG), optical heterodyne detected-optical Kerr effect (OHDOKE), and Z-scan methods.<sup>1,7</sup> As an example, a brief description of the Z-scan technique, which is one of the most common techniques for RSA-based optical limiting studies of Pcs, is presented. This method has been used to determine the sign and the magnitude of both the real and imaginary parts of third-order nonlinear optical susceptibility  $\{\chi^{(3)}\}$ .<sup>24</sup> The real part can be assigned as the nonlinear refractive index of the material, whereas the imaginary part represents the nonlinear absorption coefficient. In the experimental apparatus a single laser beam in a tight focus geometry is used (Fig. 3). The relative transmission (ratio  $D_2/D_1$ ) of a nonlinear medium is recorded as a function of the sample position  $z$ , measured with respect to the focal plane of the incident beam. Increasingly larger values for both nonlinear refraction and nonlinear absorbance are usually obtained for higher intensity irradiation of the material. Hence, it is obvious that considerable nonlinear responses are observed as the sample crosses the focal plane of the beam ( $z = 0$ ). Depending

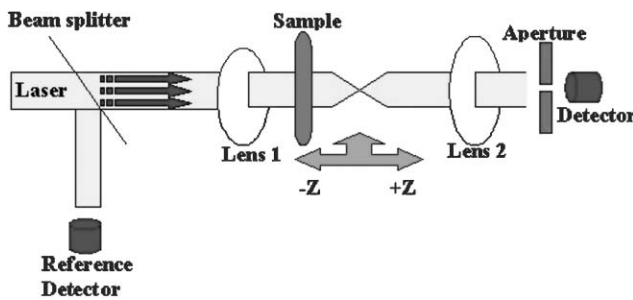


Fig. 3 Experimental apparatus used for Z-scan measurements.

on whether there is an aperture or not, two different basic experiments can be performed with the experimental apparatus shown in Fig. 3. The presence of an aperture at the exit lens ( $A_2$ ) makes the experiment sensitive to both nonlinear absorption and nonlinear refraction. With the aperture removed, and all the transmitted light collected onto the detector, the sensitivity to nonlinear refraction is completely eliminated. In this case, changes in the relative transmission are due to nonlinear absorption only. Fig. 4 shows a typical open aperture Z-scan (curve a) of a material with a positive nonlinear absorption coefficient. The strongest absorption is found when the sample crosses the position  $z = 0$ , thus demonstrating how the irradiance symmetrically increases to a maximum value located about the focal plane. This situation is found for RSA or multiphoton absorption. The opposite effect, *i.e.* SA (curve b in Fig. 4), is found for materials with a negative nonlinear absorption coefficient: the relative transmission increases and has a maximum in the focal plane.

In an open aperture Z-scan experiment, by moving the sample along the  $z$ -axis through the focus the intensity-dependent absorption is measured as the change of the transmission through the sample using a detector in the far field. On approaching the focus the intensity increases by several orders of magnitude relative to the intensity away from focus, inducing nonlinear absorption in the sample. Absorption coefficients are calculated by fitting the theory reported by Sheik-Bahae *et al.*<sup>24</sup> The normalized transmittance

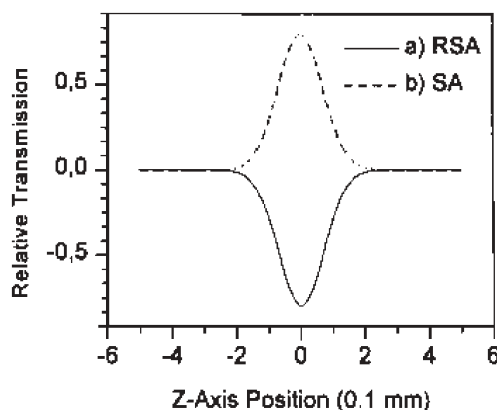


Fig. 4 Open aperture Z-scan, relative transmission as a function of the sample position  $z$ ; nonlinear absorption coefficient of the material is: (a) positive, (b) negative.

as a function of position  $z$ ,  $T_{\text{Norm}}(z)$  is given by

$$T_{\text{Norm}}(z) = \sum_{i=0}^{\infty} \left( \frac{[-q_0(z, 0)]^i}{(i+1)^{3/2}} \right) \quad (1)$$

where  $q_0(z)$  is given by

$$q_0(z) = \frac{q_{00}}{1 + (z/z_0)^2} \quad (2)$$

In (2),  $z_0$  is the diffraction length of the beam and  $q_{00} = \beta^{(3)} I_0 L_{\text{eff}}$  where  $L_{\text{eff}} = [1 - \exp(-z_0 L)]/z_0$ ,  $\beta^{(3)}$  is the third order nonlinear absorption coefficient,  $I_0$  is the intensity of the light at focus and  $L_{\text{eff}}$  is known as the effective length of the sample, defined in terms of the linear absorption coefficient,  $z_0$ , and the true optical path length through the sample,  $L$ .

The imaginary third-order susceptibility  $\text{Im}\{\chi^{(3)}\}$  and the second-order hyperpolarizability  $\gamma$  are used to quantify the nonlinear absorption.  $\text{Im}\{\chi^{(3)}\}$  is directly related to the third order absorption coefficient  $\beta^{(3)}$  and is expressed as

$$\text{Im}\{\chi^{(3)}\} = \frac{n_0^2 \epsilon_0 c \lambda \beta^{(3)}}{2\pi} \quad (3)$$

where  $n_0$  is the linear refractive index,  $\epsilon_0$  is the permittivity of free space,  $c$  is the speed of light and  $\lambda$  is the wavelength of the incident light. The relationship between  $\text{Im}\{\chi^{(3)}\}$  and  $\gamma$  is defined as:

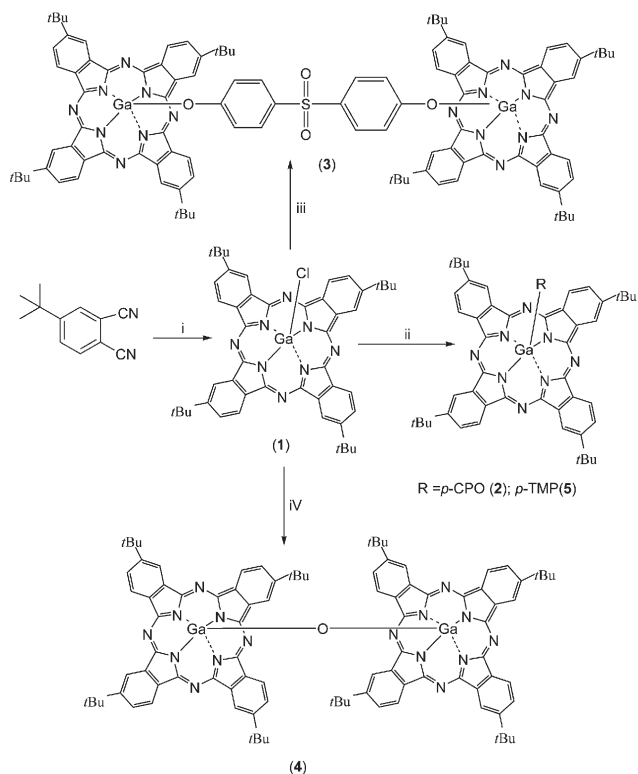
$$\gamma = \frac{\text{Im}\{\chi^{(3)}\}}{f^4 c_{\text{mol}} N_A} \quad (4)$$

where  $f = (n_0^2 + 2)/3$  is the Lorentz local field factor,  $n_0$  is the linear refractive index of the sample,  $c_{\text{mol}}$  is the molar concentration and  $N_A$  is Avagadro's number.

#### 4. Axially modified gallium phthalocyanines

It is known that the disadvantage of peripherally unsubstituted phthalocyanines is their poor solubility in organic solvents. To overcome this problem, a variety of substituents, for example, alkoxy, alkyl, aryl, F,  $\text{CF}_3$  and others, have been attached to the macrocycle, in varying numbers and different substitution patterns. The graft of alkoxy groups into the  $\alpha$ -positions of both Pcs and naphthalocyanines (Ncs) is shown to be a very useful method for tuning the spectral range of the optical limiter. The peripherally electron-withdrawing groups substituted phthalocyanines exhibit good optical limiting performances. In comparison with octasubstituted phthalocyanine, tetrasubstituted phthalocyanine exhibits much higher solubility mainly due to a lower degree of order in the solid state, which facilitates salvation by the more pronounced interaction with solvent molecules. Also, the less symmetric isomers possess a higher dipole moment caused by the more asymmetric arrangement of the substituents in the periphery of the macrocycle. Tetra(*tert*-butyl)-substituted Pcs and their metal complexes are the most frequently used when solubility is required.

Peripherally unsubstituted galliumphthalocyanines with an axial chloro, fluoro and hydroxy ligand ( $\text{PcGaX}$ ,  $\text{X} = \text{Cl}, \text{F}, \text{OH}$ ) have been studied in detail.<sup>8</sup> In recent years we have concentrated our efforts on studying the influence of different axial substituents on the NLO properties, particularly on the OL properties of soluble peripherally alkyl-substituted indium, gallium and titanium Pcs and Ncs.<sup>7b</sup> Scheme 1 gives the synthetic routes of  $t\text{Bu}_4\text{PcGaCl}$  (**1**),<sup>25,26</sup>  $[\text{tBu}_4\text{PcGa}(p\text{-CPO})]$  (*p*-CPO = *p*-chlorophenoxy) (**2**),<sup>27</sup>  $[\text{tBu}_4\text{PcGa}]_2\text{SDPO}$  (SDPO = 4,4'-sulfonyldiphenoxyl) (**3**),<sup>27</sup>  $[\text{tBu}_4\text{PcGa}]_2\text{O}$  (**4**)<sup>28</sup> and  $t\text{Bu}_4\text{PcGa}(p\text{-TMP})$  [*p*-TMP = *p*-trifluoromethylphenyl] (**5**).<sup>25,26</sup> In comparison with **1**, compounds **2**–**4** were found to be more soluble in many common organic solvents—even in methanol and acetone. EXAFS analysis for **4** indicated that the distance between Ga and bridging oxygen atom was found to be 1.87 Å.<sup>29</sup> The inter-Pc distance in **4** is thus about 3.72 Å, which is in the quite good agreement with the reported value (3.8 Å) obtained from the theoretical calculation for the minimized structure of **4**.<sup>30</sup> When a rigid phthalocyanine molecule, which is not deformed by the metal atom is assumed, the shortest metal atom and nitrogen distance amounts to 1.97 Å. The gallium center is located 0.45 Å out of the plane described by the four nitrogen atoms directly bonded to it. Table 1 and Fig. 5 give the EXAFS data and molecular structure of  $[\text{tBu}_4\text{PcGa}]_2\text{O}$ . The dipole moment value of **4** is very small (only 0.3 Debye) when compared to those of compounds **1** and **5** (6.6 D for **1** and 4.9 D for **5**); however, this



**Scheme 1** Synthesis of gallium phthalocyanines **1**–**5**: (i)  $\text{GaCl}_3$ , quinoline, DBU, 180 °C, 7 h, 68%; (ii) anhydrous DMSO, *p*-chlorophenol,  $\text{K}_2\text{CO}_3$ , 110 °C, 14 h, 87% for **2**; (*p*-TMP)MgBr, THF, r.t., 77% for **5**; (iii) dry DMSO, 4,4'-sulfonyldiphenol,  $\text{K}_2\text{CO}_3$ , 110 °C, 10 h, 40%; (iv) conc.  $\text{H}_2\text{SO}_4$ , –10 to –20 °C, 2 h, 72%.

**Table 1** EXAFS determined structural data of **4** measured at Ga K-edge

	$N^a$	$r [\text{\AA}]^b$	$\sigma [\text{\AA}]^c$
Ga–O	1	$1.87 \pm 0.02$	$0.052 \pm 0.005$
Ga–N <sub>pyrrol</sub>	4	$2.02 \pm 0.02$	$0.057 \pm 0.006$
Ga–C	8	$3.01 \pm 0.03$	$0.062 \pm 0.013$
Ga–N <sub>aza</sub>	4	$3.33 \pm 0.04$	$0.088 \pm 0.026$
Ga <sub>(out)</sub> [Å] <sup>d</sup>	0.45 ± 0.09		

<sup>a</sup> N: coordination number. <sup>b</sup> r: interatomic distance between the absorber and the backscatterers. <sup>c</sup>  $\sigma$ : Debye–Waller factor with calculated standard deviations. <sup>d</sup> Ga<sub>(out)</sub>: the out of plane displacement of the Ga atom.

dimer exhibits a higher Hyper Raleigh Scattering value ( $\beta_{\text{HRS}}$ ) at 1064 nm ( $86 \times 10^{-30}$  esu) with respect to monomeric **Pc 1** and **5** as a result of the higher number of  $\pi$ -electrons distributed in two planes, which are in this case closely spaced.<sup>30</sup>

The electronic absorption spectra of phthalocyanines are characterized by intense Q-band in the red end of the visible spectrum of light between 600–700 nm, and a less intense B-band at 300–400 nm in the blue end of the visible spectrum. The transitions can be understood through the work on the electronic structure of Pcs by Gouterman *et al.*<sup>31</sup> The UV/Vis spectra of **2** and **3** are almost identical. Unlike the axially aryl-substituted gallium phthalocyanine **5**, whose Q and B-bands in the UV/Vis spectra are shifted to the red by a few nanometers relative to **1**, axially aryloxy substitution at central gallium atom gives rise to a weak (2–3 nm) blue shift of the Q-band of compounds **2** and **3**. The  $\mu$ -oxo-bridged gallium phthalocyanine dimer **4** exhibits a similar result.

Compounds **2**–**5** show the more intense photoluminescence emission in the red region compared to the monomeric complex **1**.<sup>28</sup> Fig. 6 gives an example for the typical steady-state absorption and fluorescence spectra of **3** in anhydrous toluene. For all compounds, steady-state fluorescence spectra ( $\lambda_{\text{ex}} = 410$  nm) show the mirror image of the corresponding UV/Vis absorption bands with small Stokes-shifts, implying that the structure change between the ground state and excited singlet state is small. The values of fluorescence lifetime ( $\tau_f$ ) of the  $\text{PcGa}$  derivatives are the order of ns. Compared with monomers, the  $\mu$ -oxo- and SDPO- bridged dimers exhibit longer  $\tau_f$  values. Upon excitation with a nanosecond laser at 355 nm, transient absorption spectra observed in toluene are similar for all samples. The transient absorption bands appear at ~520 nm with the depletion of the ground state absorptions of phthalocyanine in the region of 620–720 nm, and are easily quenched in the presence of a triplet energy quencher such as oxygen. The transient absorption band at ~520 nm can thus be assigned to the transition from the lowest triplet excited state to the upper triplet excited states (T–T absorption). Among these compounds, compound **3** exhibits the longest triplet excited state lifetime, up to 667  $\mu\text{s}$ .<sup>32</sup> It is interesting to note that for all samples, the triplet-state maximum occurs in the region of 400–610 nm, which is just located inside the high-transmittance region between the intense Q and B bands in the UV/Vis spectra of the samples. This implies that the absorption cross section of the excited-state is always larger than that of the ground-state in this region.

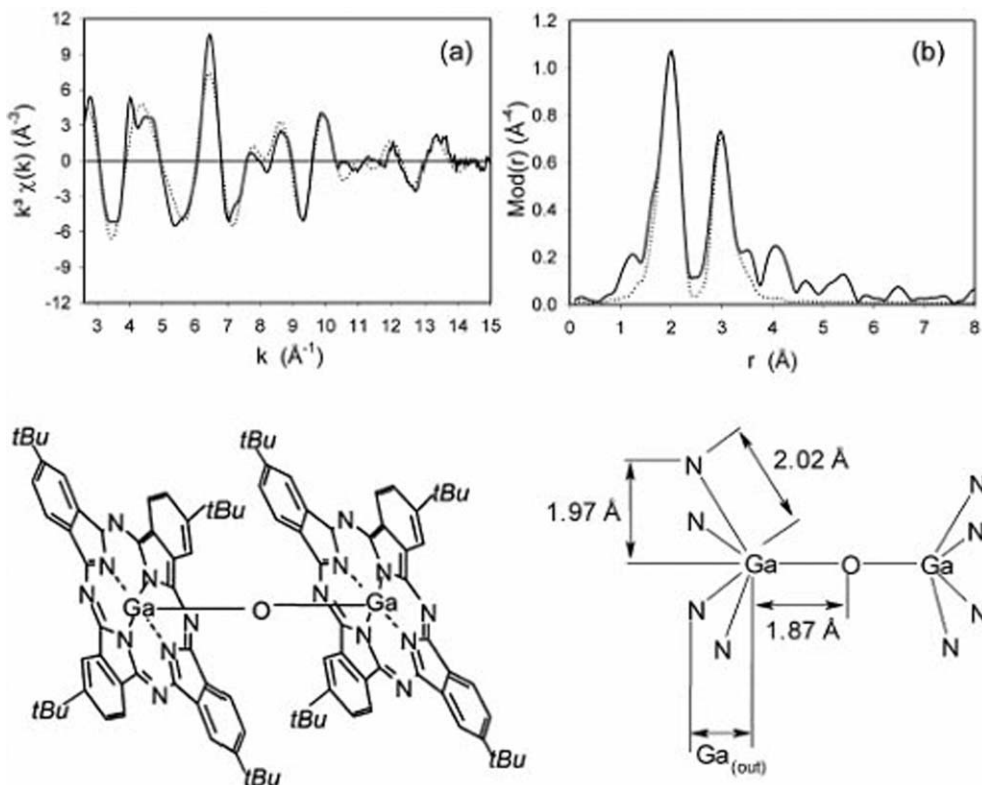


**Fig. 5** Experimental (solid line) and calculated (dotted line)  $k^3 \chi(k)$  functions (a) and their Fourier transforms (b) for **4** measured at Ga K-edge ( $k$  range: 2.6–15.0  $\text{\AA}^{-1}$ ,  $\Delta E_0$ : 14.69 eV, fit index: 33.57) (upper panel); EXAFS determined molecular structure of **4** (lower panel).

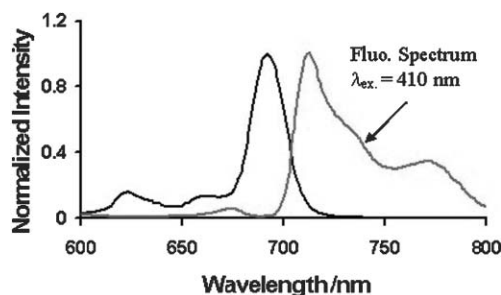


**Fig. 6** The steady-state absorption and fluorescence spectra of **3** in  $\text{CHCl}_3$ .

The open aperture of a Z-scan experiment was used to measure the NLO response in the samples. All Z-scans performed for compounds exhibit a decrease of transmittance about the focus typical of an induced positive nonlinear absorption of incident light. In Fig. 7 the experimentally determined values of  $\text{Im}\{\chi^{(3)}\}$  are plotted as a function of the focal intensity. Each data point on the plot represents an independent open aperture Z-scan of the compound in question and the solid lines are sketched merely as guides to the eye. It can clearly be seen that  $\text{Im}\{\chi^{(3)}\}$  tends to reduce in magnitude with increasing focal intensity  $I_0$  in the figure. This, coupled with the fact that the closed aperture Z-scans (nonlinear refraction) did not exhibit pure third effects either, leads to the only conclusion that the absorption effects were a combination of third and higher odd order nonlinear

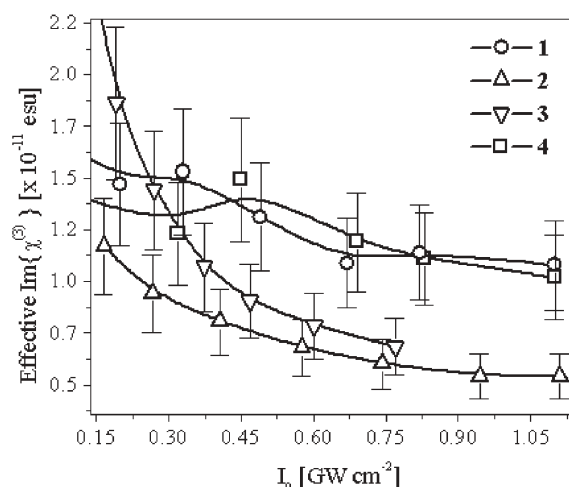


**Fig. 7** Plot of effective  $\text{Im}\{\chi^{(3)}\}$  against the on focus beam intensity  $I_0$  for compounds **1–4** at  $0.5 \text{ g L}^{-1}$  in toluene. Each data point represents an independent open aperture Z-scan and the solid lines are intended as guides to the eye.

absorptions. Despite this, effective third order nonlinear susceptibilities ( $\text{Im}\{\chi^{(3)}_{\text{eff}}\}$ ) were estimated by suitably interpolating the data in Fig. 7 for all four compounds at on focus intensities of  $0.5 \text{ GW cm}^{-2}$  (arbitrarily chosen). Subsequently  $\text{Im}\{\chi^{(3)}_{\text{eff}}\}$  and molecular second hyperpolarizabilities  $\gamma_{\text{eff}}$  were determined for compounds **1–5** for this sample  $I_0$  value. All calculated coefficients are given in Table 2.

**Table 2** Summary of the nonlinear optical properties for gallium phthalocyanines **1–6**

Samples	C (g L <sup>-1</sup> )	$\alpha_0$ (cm <sup>-1</sup> )	Im{ $\chi^{(3)}$ <sub>eff</sub> } ( $\times 10^{-11}$ esu)	$\gamma_{\text{eff}}$ ( $\times 10^{-32}$ esu)	$\kappa$ ( $\sigma_{\text{ex}}/\sigma_0$ )	$F_{\text{sat}}$ (J.cm <sup>-2</sup> )	$\omega_0$ (μm)
<b>1</b>	0.5	1.10	1.20 ± 0.2	0.84 ± 0.1	13.5 ± 0.4	27.0 ± 1.0	23
<b>2</b>	0.5	1.37	0.88 ± 0.2	0.69 ± 0.1	9.5 ± 0.4	16.3 ± 0.9	25
<b>3</b>	0.5	3.13	0.73 ± 0.1	1.13 ± 0.2	4.8 ± 0.6	7.5 ± 0.8	31
<b>4</b>	0.5	1.60	1.30 ± 0.2	1.76 ± 0.3	11.3 ± 0.1	13.5 ± 1.0	23
<b>5</b>	0.5	0.91	1.10 ± 0.2	0.86 ± 0.1	13.6 ± 0.4	8.4 ± 1.0	23
<b>6</b>	0.5	1.30	1.30 ± 0.2	2.10 ± 0.3	10.4 ± 0.3	8.9 ± 0.4	25

The open aperture spectra were manipulated and replotted with the normalized transmission ( $T_{\text{Norm}}$ ) against the incident energy density per pulse (J cm<sup>-2</sup>) to further investigate the optical limiting. The nonlinear absorption coefficient  $\alpha(F, F_{\text{Sat}}, \kappa)$  was used to fit the normalized transmission as a function of this energy density to a superposition of all open aperture datasets for each compound.<sup>7a</sup> The symbols  $F$ ,  $F_{\text{Sat}}$  and  $\kappa$  represent the incident energy density per pulse, the saturation energy density and the ratio of the excited to ground state absorption cross section  $\sigma_{\text{ex}}/\sigma_0$ , respectively. The method of least square regression was employed, where the parameters  $\kappa$  (realistically  $\sigma_{\text{ex}}$  as  $\sigma_0$  was measured) and  $F_{\text{Sat}}$  were treated as free constants in the fitting algorithm. The fitting converged with  $R^2$  values in the region of 0.99 in all cases. The plots of normalized transmission against pulse energy density for compounds **1–4** where the solid lines are theoretical fits to the experimental data are shown in Fig. 8.

Compound **5** exhibits the largest excited to ground state absorption cross section ratio  $\kappa \approx (13.6 \pm 0.4)$  and it also possesses the lowest linear absorption coefficient  $\alpha_0 \approx 0.91 \text{ cm}^{-1}$  of the series **1–5**. The  $\kappa$  coefficient for compound **3** is the lowest of the series at (4.8 ± 0.6) while its linear absorption coefficient,  $\alpha_0 \approx 3.13 \text{ cm}^{-1}$ , is the highest of the four compounds by a factor of 2–3 when compared to the linear absorption of compounds **1**, **2** and **4**, **5**. The relatively large linear absorption coefficient is therefore responsible for the significant reduction in the  $\kappa$  coefficient when the chlorogallium phthalocyanine monomer **1** is substituted with a *p*-CPO group at the axial position. The magnitude of the

nonlinear absorption coefficient (directly proportional to  $\text{Im}\{\chi^{(3)}\}$ ) is lowest for compound **3** and largest for compound **4** under 0.5 GW cm<sup>-2</sup> irradiation. Thus, dimerisation of the gallium phthalocyanine monomer resulted in producing compounds with both the largest and smallest nonlinear absorption coefficient in the study.

The  $F_{\text{Sat}}$  values for compounds **1–5** range from (7.5 ± 0.8) J cm<sup>-2</sup> for **3** to (27.0 ± 1.0) J cm<sup>-2</sup> for **1**. Thus, while compound **3** exhibited the lowest nonlinear absorption coefficient it also saturated at the lowest energy density indicating that dimerisation of the gallium phthalocyanine monomer in this way results in a compound that saturates at an energy density 3.6 times lower than compound **1**. The saturation energy density was reduced by a factor ≈ 1.7 by the addition of the *p*-CPO at the axial position (compound **2**), by a factor ≈ 2 by dimerisation with a μ-oxo-bridge (compound **4**), and by a factor ≈ 3.2 by substitution of the *p*-TMP group (compound **5**) when compared to the saturation energy density of chlorogallium monomer (compound **1**). The ability to control reductions in the saturation energy density is important from the point of view of realizing applications where one would require successive layers in the practical limiter to be fabricated from materials of decreasing saturation energy density.

It is worth considering the waist radius of the beam as determined from the fitting of the open aperture spectra. Compound **3** exhibited the largest waist radius ( $\omega_0 \approx 31 \mu\text{m}$ ) of the beam the four compounds with compounds **1**, **2**, **4**, **5** exhibiting waist radius  $\omega_0 \approx 23 \mu\text{m}$ , 25 μm, 23 μm and 23 μm respectively. Dimerisation of compound **1** into compound **3** therefore resulted in larger refraction in the sample enlarging the waist radius of the focused beam by a factor ~1.3. This is a desirable effect in practical optical limiters as it reduces the energy density of the incident pulses.

## 5. Gallium phthalocyanine dimer with a direct Ga–Ga bond

The synthesis and molecular structure of organogallium compounds with gallium–gallium bond are an interesting area. A number of novel organogallium compounds with gallium–gallium bond, for examples,  $\text{Ga}_2\text{R}_2(\mu\text{-O}_2\text{CCH}_3\text{-O},\text{O}')$ <sub>2</sub> [R =  $\text{CH}(\text{SiMe}_3)_2$ ,<sup>33</sup>  $[\text{Ga}_2\text{Cl}_4(\text{dioxane})_2]_x$ ,<sup>34</sup>  $[(\text{Me}_3\text{Si})_2\text{C}(\text{Ph})\text{C}(\text{Me}_3\text{Si})\text{NGaCl}]_2$ ,<sup>35</sup> and  $[(\text{Me}_3\text{Si})_2\text{HC}]_4\text{Ga}_2$ ,<sup>36</sup> have been reported so far. Very recently, Bertagnoli and Chen *et al.* reported on the synthesis, structural characterization and nonlinear optical properties of a gallium phthalocyanine dimer with a direct gallium–gallium bond<sup>37</sup> *i.e.*,  $[\text{tBu}_4\text{PcGa}]_2\text{.2dioxane}$  (**6**). This dimer is prepared with 83%

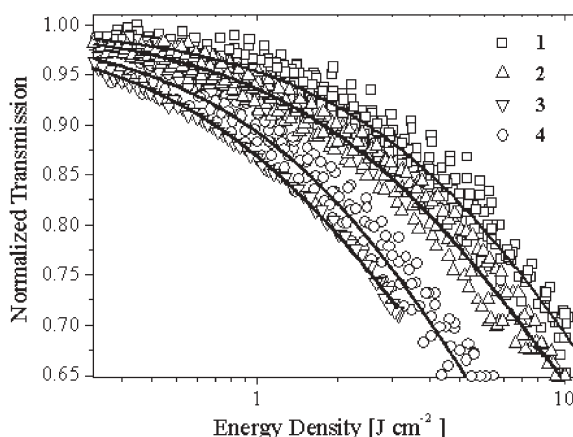


**Fig. 8** Plot of normalized transmission against pulse energy density for compounds **1–4** at 0.5 g L<sup>-1</sup> in toluene where the solid lines are theoretical fits to the experimental data. The fitting parameters are given in Table 2.

yield by the reaction of soluble  $t\text{Bu}_4\text{PcGaCl}$  with activated magnesium in freshly dried THF and in the presence of 1,4-dioxane. The formation of the gallium–gallium bond in  $[\text{tBu}_4\text{PcGa}]_2\text{.2dioxane}$  was initially confirmed by EXAFS spectroscopy. The gallium–gallium distance was found to be 2.46 Å, which is in good agreement with the reported Ga–Ga bond lengths in some organogallium compounds.<sup>33–36</sup> The Gallium center is located 0.45 Å out of the plane of Pc macrocycle. This value is close to the reported out-of-plane value of 0.439 Å in crystalline  $\text{PcGaCl}$ .<sup>38</sup> Fig. 9 give the EXAFS determined molecular structure of  $[\text{tBu}_4\text{PcGa}]_2\text{.2dioxane}$ .

The similarity of the UV-vis spectra of  $t\text{Bu}_4\text{PcGaCl}$  (**1**) and  $[\text{tBu}_4\text{PcGa}]_2\text{.2dioxane}$  (**6**)<sup>37</sup> implies that the two Pc rings in the Ga–Ga bridged dimer do not greatly modify the electronic distribution of each other. The extent of electronic conjugation in both compounds is practically the same since dimer **6** has a gallium–gallium single bond of  $\sigma$ -type with no presence of delocalized electrons. As expected, the main differences between the spectral features of **1** and **6** are related to the change of the molar extinction coefficient due to the different number of absorbing Pc rings per molecular unit in passing from the monomer to the Ga–Ga bridged dimer. Photoluminescence spectra ( $\lambda_{\text{ex}} = 355$  nm) of **1** and **6** in dilute chloroform solutions showed that, upon emission both compounds display a Stokes shift of the emission peak with respect to the location of the Q-band absorption. Different to absorption spectra, dimerization influences more strongly the energy of emission, since the extent of Stokes shift is larger for the monomer with respect to the dimer. Maximum emission peaks for **1** and **6** are found at 713 nm and 700 nm, respectively. Such a difference could be ascribed to the more rigid structure of the dimer with respect to the monomer. This means that the dimer relaxes radiatively from the electronic excited state  $\pi^*$  in a higher vibrational level.

Z-scan experiments show that, compound **6** exhibits a significantly lower  $F_{\text{Sat}}$  than that of **1**, by approximately a factor of 3. The ratio of their excited and ground state absorption cross sections is similar to **1** exhibiting a  $\kappa$  coefficient approximately 1.35 times that of **6**. Thus dimerization of **1** is clearly a viable method of tuning the saturation energy density ( $F_{\text{Sat}}$ ) of the material, reducing it by a factor of

3. This reduction in  $F_{\text{Sat}}$  is coupled with a slight increase of  $\beta_1$  at low incident intensity and with approximately equivalent  $\beta_1$ 's at higher intensities. The  $\kappa$  coefficient is reduced by approximately 22% after dimerization of **1** to **6** but this can probably be mostly attributed to the increase linear absorption coefficient by approximately 18% over the same molecular modification.

In our previous paper, we described the preparation of the first dimeric indium phthalocyanine complex with an indium–indium bond  $[\text{tBu}_4\text{PcIn}]_2\text{.2tmed}$  by a Wurtz coupling reaction of  $t\text{Bu}_4\text{PcInCl}$  in the presence of *N,N,N',N'*-tetramethylethylene diamine (tmed).<sup>39</sup> By EXAFS measurements the In–In distance was found to be 3.24 Å. Similar to the results presented for  $[\text{tBu}_4\text{PcGa}]_2\text{.2dioxane}$  we found that dimerization of the  $t\text{Bu}_4\text{PcInCl}$  reduced the  $F_{\text{Sat}}$  by a factor of approximately 2.5 (comparable to a factor approximately 3 for **6**). The In–In Pc dimer also exhibited a slightly lower  $F_{\text{Sat}}$  ( $24.2 \pm 0.8 \text{ J cm}^{-2}$ ) than that of compound **6**. The reduction of  $\kappa$  for the monomeric  $t\text{Bu}_4\text{PcInCl}$  by a factor of about 2.2 after dimerization is far more significant than the reduction by a factor of 1.3 for the Ga compounds presented here. This difference can be partially attributed to the particularly low linear absorption coefficient of the  $t\text{Bu}_4\text{PcInCl}$  molecule, which allows it exhibit a large  $\kappa$  coefficient compared to other Pcs.<sup>7a</sup>

## 6. Axially modified gallium naphthalocyanines

The influence of the extension of the  $\pi$ -electron conjugation on the NLO response has been studied by Nalwa *et al.*<sup>40,41</sup> The results show that third-order optical nonlinearity increases with the enlargement of the  $\pi$ -electron conjugation. In contrast to phthalocyanines, naphthalocyanines (Ncs) are almost transparent in the red light region; they have transmission windows in the yellow and red region of the spectrum. However, too much research work is mainly focused on phthalocyanines rather than naphthalocyanine compounds probably due to their much higher tendency to aggregate and thus lower solubility, and due to the more pronounced sensitivity of Ncs towards oxidation. Strategies to solubilize Ncs thus involve the formation of tetra- or octasubstituted Ncs carrying alkyl- or alkoxy substituents.

### 6.1 Peripherally tetra(*tert*-butyl)-substituted gallium naphthalocyanines

Peripherally unsubstituted gallium(III) naphthalocyanines, *e.g.*  $\text{NcGaCl}$ ,  $\text{NcGa(OH)}$ ,  $\text{NcGaOSi}(\text{n-C}_6\text{H}_{13})_3$ ,  $(\text{NcGaF})_n$  have been reported,<sup>42</sup> however, these compounds have very poor solubility in common organic solvents. To combine all the requirements for a good optical limiter with such properties like high solubility and stability, we synthesized the soluble axially monosubstituted gallium naphthalocyanines:  $t\text{Bu}_4\text{NcGaCl}$  (**7**),  $t\text{Bu}_4\text{NcGa}(p\text{-TMP})$  (**8**), and the  $\mu$ -oxo-bridged naphthalocyanine  $[\text{tBu}_4\text{NcGa}]_2\text{O}$  (**9**) very recently (Scheme 2).<sup>43</sup> In comparison with the corresponding gallium phthalocyanine compounds:  $t\text{Bu}_4\text{PcGaCl}$  (**1**),  $t\text{Bu}_4\text{PcGa}(p\text{-TMP})$  (**5**), and  $[\text{tBu}_4\text{PcGa}]_2\text{O}$  (**4**) described before, all gallium naphthalocyanines **7–9**, especially compound **7**,

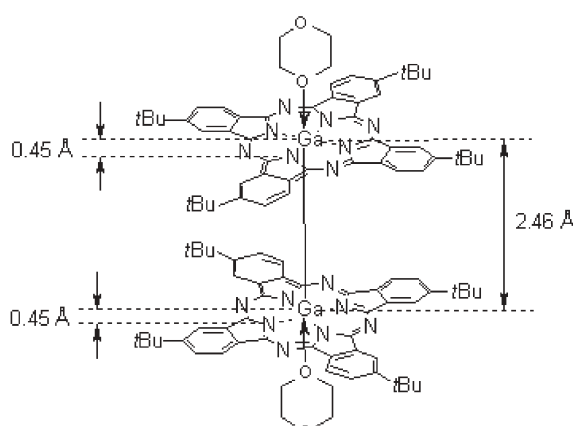
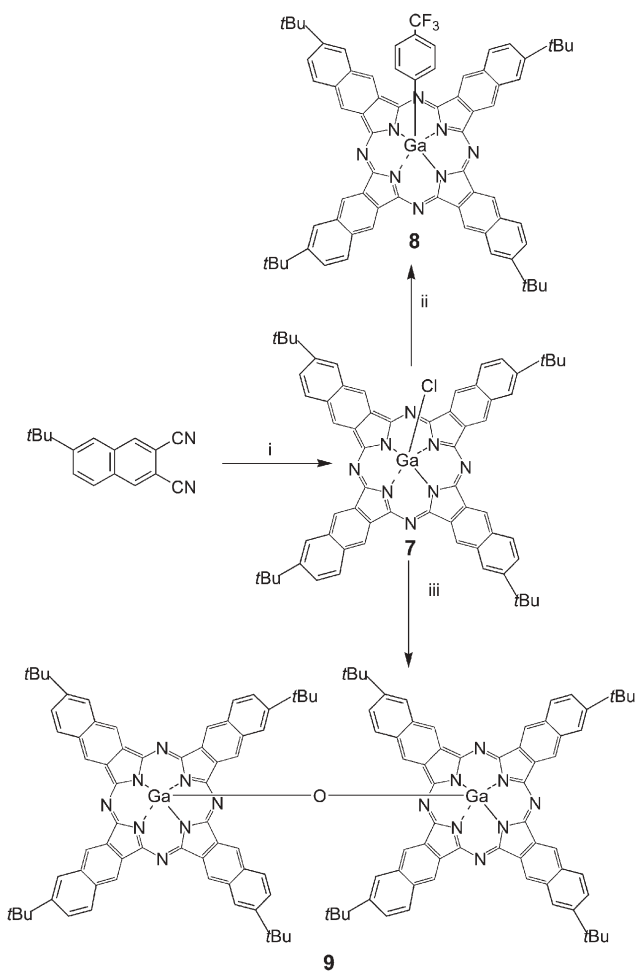


Fig. 9 EXAFS determined molecular structure of **6**.



**Scheme 2** Synthesis of gallium naphthalocyanines **7–9**: (i)  $\text{GaCl}_3$ , quinoline, DBU,  $180\text{ }^\circ\text{C}$ , 46%; (ii) (*p*-TMP)MgBr (excess), THF, r.t., 77%; (iii) 96%  $\text{H}_2\text{SO}_4$ ,  $-20\text{ }^\circ\text{C}$ ; 2 h, 76%.

showed a somewhat stronger tendency to aggregate in solutions, especially at high concentration.

The observed transient absorption bands in the 500–700 nm with a peak maximum at 600 nm were attributed to the triplet-triplet (T–T) transition.<sup>43</sup> In comparison to the corresponding gallium phthalocyanines,<sup>25,27,28</sup> gallium naphthalocyanines have their T–T bands red-shifted about 80 nm. It should be noted that these T–T absorption bands are located inside the high-transmittance region between the intense Q and B bands in the UV/Vis spectra of all samples. After the laser exposure, the T–T absorption begins to decay for a hundred microseconds. The decay of the T–T absorption was curve-fitted

with a single exponential when the laser power was employed. As can be seen from Table 3, the lifetimes of the triplet states are in the region of 13.8–21.4  $\mu\text{s}$ , which are shorter than those of gallium phthalocyanine compounds,<sup>26,28</sup> but longer than the nanosecond laser employed in the optical limiting measurements. The observation of the T–T absorption in microsecond region suggests that the fluorescence decay is mainly attributed to the intersystem crossing from the lowest singlet excited state to the lowest triplet state. All Z-scans for **7–9** exhibit a decrease of transmittance about the focus typical of an induced positive nonlinear absorption of incident light. These compounds optically limit at sufficiently high intensity *via* a RSA mechanism into the excited T–T absorption band at 532 nm excitation.

The optical limiting properties of these materials mentioned above are investigated (Fig. 10).<sup>43</sup> The  $F_{\text{Sat}}$  values of **7** and **9** follow the same trend as their phthalocyanine analogues **1** and **4**, with the dimer having a lower value than that of the monomer for both species of compound (see Table 4). In the **7–9** cases the numerical values of  $F_{\text{Sat}}$  are much closer than in the  $t\text{Bu}_4\text{PcGa}$  case. The magnitude of  $F_{\text{Sat}}$  is also changed significantly from the gallium phthalocyanine case where **1** and **4** have  $F_{\text{Sat}}$  values  $\approx 27 \pm 1.0 \text{ J cm}^{-2}$  and  $13.5 \pm 1.0 \text{ J cm}^{-2}$ , respectively, while the corresponding naphthalocyanines **7**, **9** have  $F_{\text{Sat}} \approx 5.6 \pm 0.2 \text{ J cm}^{-2}$  and  $3.9 \pm 0.2 \text{ J cm}^{-2}$ , respectively. In contrast to the axially *p*-TMP substituted gallium phthalocyanine **5**, the saturation density  $F_{\text{Sat}}$  for the axially *p*-TMP substituted gallium naphthalocyanine **8** does

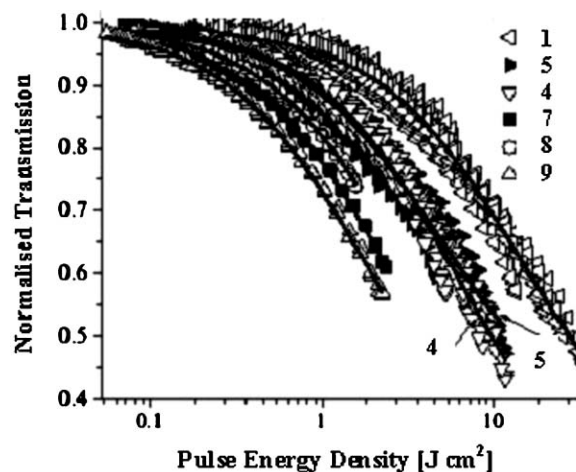


**Fig. 10** Plots of normalized transmission against incident pulse energy density for gallium naphthalocyanines **7–9** and gallium phthalocyanines **1**, **4** and **5**.

**Table 3** Photophysical properties of compounds **1**, **3**, **4**, **5**, **7**, **8**, **9** in deaerated anhydrous toluene.  $\tau_{\text{fluo}}$ : fluorescence lifetimes at emission peak wavelength,  $\lambda_{\text{ex}} = 410\text{ nm}$ ;  $\tau_{\text{T}}$ : triplet state lifetime,  $\lambda_{\text{ex}} = 355\text{ nm}$ ;  $\lambda_{\text{T-T}}$ : T–T absorption maxima

Samples	$\lambda_{\text{max}}^{\text{abs}}$ (nm)	$\lambda_{\text{max}}^{\text{fluo}}$ (nm)	$\tau_{\text{fluo}}$ (ns)	$\lambda_{\text{T-T}}$ (nm)	$\tau_{\text{T}}$ ( $\mu\text{s}$ )
$t\text{Bu}_4\text{NcGaCl}$ ( <b>7</b> )	805	830	1.89	600	21.4
$t\text{Bu}_4\text{NcGa}(p\text{-TMP})$ ( <b>8</b> )	806	828	1.79	600	18.2
$[t\text{Bu}_4\text{NcGa}]_2\text{O}$ ( <b>9</b> )	803	824	2.33	600	13.8
$t\text{Bu}_4\text{PcGaCl}$ ( <b>1</b> )	693	702	2.57	520	257
$t\text{Bu}_4\text{PcGa}(p\text{-TMP})$ ( <b>5</b> )	696	701	2.48	520	200
$[t\text{Bu}_4\text{PcGa}]_2\text{O}$ ( <b>4</b> )	692	701	3.57	520	357
$[t\text{Bu}_4\text{PcGa}]_2\text{SDPO}$ ( <b>3</b> )	692	712	3.46	520	667

**Table 4** Summary of the nonlinear optical properties for gallium naphthalocyanines **7–9**

Samples	C (g L <sup>-1</sup> )	$\alpha_0$ (cm <sup>-1</sup> )	Im{ $\chi^{(3)}$ } ( $\times 10^{-11}$ esu)	$\gamma$ ( $\times 10^{-32}$ esu)	$\kappa$ ( $\sigma_{\text{ex}}/\sigma_0$ )	$F_{\text{Sat}}$ (J.cm <sup>-2</sup> )
<i>t</i> Bu <sub>4</sub> NcGaCl ( <b>7</b> )	0.5	4.4	3.0 $\pm$ 0.6	1.52 $\pm$ 0.3	4.8 $\pm$ 0.2	5.6 $\pm$ 0.2
<i>t</i> Bu <sub>4</sub> NcGa( <i>p</i> -TMP) ( <b>8</b> )	0.5	2.3	2.0 $\pm$ 0.4	1.12 $\pm$ 0.2	9.2 $\pm$ 0.8	8.5 $\pm$ 0.9
[ <i>t</i> Bu <sub>4</sub> NcGa] <sub>2</sub> O ( <b>9</b> )	0.5	5.0	3.9 $\pm$ 0.7	3.84 $\pm$ 0.7	4.1 $\pm$ 0.1	3.9 $\pm$ 0.2

not follow the same trend. The saturation density of **8** is larger than that of both compounds **7** and **9**; while in the case of the gallium phthalocyanine compounds **1**, **4** and **5** the saturation density of **5** is smaller than that of **1** and **4**. The ratio of the absorption cross sections  $\kappa$  for compounds **7** and **9** follow the same trend as their phthalocyanine analogues, with the monomer being larger than the dimer. **8** and its phthalocyanine analogue **5** exhibit a different trend in their response again, with the naphthalocyanines  $\kappa$  value being larger than the  $\kappa$  value of other naphthalocyanine compounds by a factor of  $\approx 2$ . This is in contrast to the compound **5** whose  $\kappa$  value was smaller than the unsubstituted monomer **1** and axially bridged dimer **4**. It is clear from Fig. 10 that the magnitude of the nonlinear absorption is not much different for the three compounds **7–9**. The differences in the magnitude of the absorption cross section ratios  $\kappa$  for these compounds are therefore dominated by the differences in their linear absorption coefficients  $\alpha_0$ . This explains why compound **8** has a  $\kappa$  value larger than the other two compounds **7** and **9** by a factor of  $\approx 2$ , despite it exhibiting the weaker nonlinear response in terms of transmission *versus* pulse energy density. Its linear absorption coefficient is significantly smaller than that for the other compounds, approximately by a factor of 2 giving it a significantly lower linear absorption cross section  $\sigma_0$ . It was found, averaging over successive scans with increasing energy per pulse, that the magnitude of  $\omega_0$  for naphthalocyanine compounds **7** and **9** was  $\approx 22.5$   $\mu\text{m}$ . Interestingly, the average value of  $\omega_0$  for the axially *p*-TMP substituted naphthalocyanine **8** was found to be  $\approx 27.9$   $\mu\text{m}$ . It is clear that the substitution of the axially *p*-TMP ligand onto the central gallium atom resulted in a defocusing of the beam relative to the other compounds. This added defocusing of the beam is important and desirable in practical optical limiters as it helps to spatially disperse the incident pulse, further reducing the energy density of that laser pulse. Physically this can help keeping the incident energy density below the damage threshold of the limiting material. Conversely though, this was not observed in the phthalocyanine series where all the compounds **1**, **4** and **5** exhibited approximately equal average  $\omega_0$  values  $\approx 23.6$   $\mu\text{m}$ .

## 6.2 Peripherally fluorinated gallium naphthalocyanines

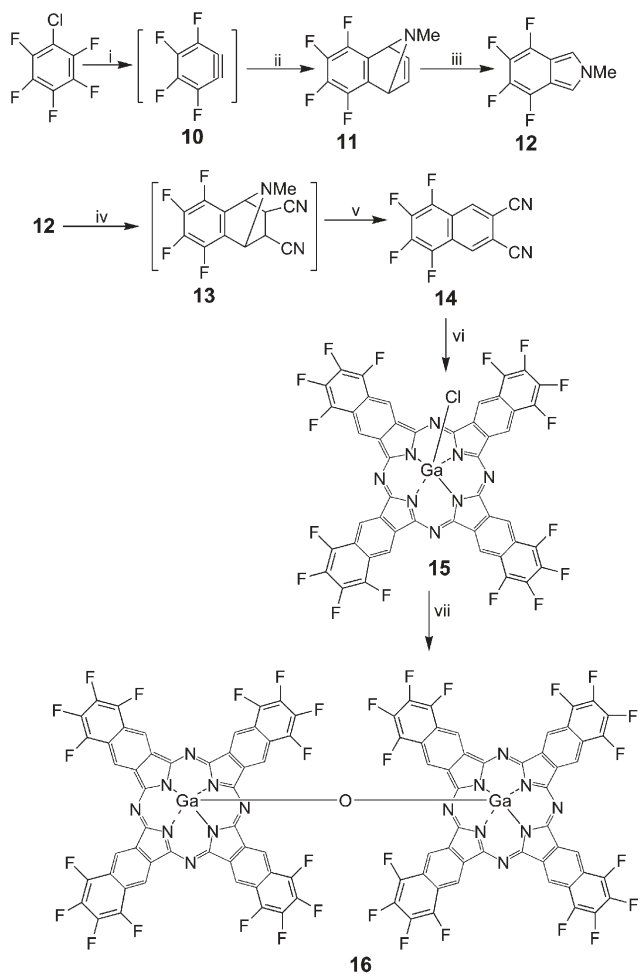
Electron-withdrawing groups in conjugated molecules are known to increase the oxidation potential of the substituted molecules thus increasing the chemical stability of these systems against, *e.g.*, oxidation due to intense light or oxygen.<sup>44</sup> The observation of the very low transmission of high intensity radiation through solutions of fluorine-substituted phthalocyanines,<sup>44</sup> *e.g.* F<sub>16</sub>PcTiO, F<sub>16</sub>PcVO, F<sub>16</sub>PcInCl and (CF<sub>3</sub>)<sub>4</sub>PcTiO, poses new different issues like the effect of fluorine on the polarizability of the electronic

cloud (nonresonant dynamic effect) under variable electric fields, and/or the modification of the optical absorption in the ground and, more important, in the excited electronic states of the substituted phthalocyanines and naphthalocyanines (molecular resonance effect). The optical limiting performance exhibited by phthalocyanines substituted with electron withdrawing atoms such as F and CF<sub>3</sub> is considerably enhanced with respect to the optical limiting effect produced by unsubstituted or differently substituted phthalocyanines. The remarkable variations of the nonlinear transmittance of perfluorinated phthalocyanines in solution indicate the strong influence that electron-withdrawing groups exhibit upon the variations of the transition dipole moments involved in the electronic transition, which effectively limits the intense radiation.<sup>44</sup>

As we discussed earlier, naphthalocyanine-based materials are also promising for optical limiting applications due to their expanded ring structure and red-shifted transmission window. In order to further improve the photostability of the electron-rich Nc rings against photoinduced oxidation, and to increase the solubility and block the aggregation of these materials, Yang *et al.*<sup>45</sup> developed a novel approach for Nc modification, namely introducing fluorine atoms on the peripheral positions of the Nc ring. **Scheme 3** gives the synthetic route for the hexadecafluorogalliumnaphthalocyanine (F<sub>16</sub>NcGaCl, **15**) and its  $\mu$ -oxo-bridged dimer ([F<sub>16</sub>NcGa]<sub>2</sub>O, **16**), which represent the first examples of peripherally fluorine-substituted naphthalocyanines. The high photostability of these two compounds is attributed to the electron-withdrawing property of the fluorine atoms, which reduce the electron density in the Nc ring and make its oxidation more difficult when irradiated. In comparison with C<sub>60</sub> and nonfluorinated NcGa compounds **7** and **9**, [F<sub>16</sub>NcG]<sub>2</sub>O displayed a better optical limiting performance, as shown in Fig. 11. The optical limiting threshold, which is defined as the average input fluence at which the output fluence is 50% of what is predicted by the linear transmission, for **16**, C<sub>60</sub>, **9** and **7** are 450, 1248, 2150, and 3945 mJ cm<sup>-2</sup>, respectively. The possible reason for the enhancement of the optical limiting behavior in **16** is probably due to the involvement of the strong electron-withdrawing nature of the fluorine substituents, improved dipole moments and a higher effective  $\sigma_{\text{ex}}/\sigma_0$  ratio.

## 7. Summary and outlook

The recent achievements on synthesis, photophysical properties and nonlinear optical (including optical limiting) properties of gallium phthalocyanines and naphthalocyanines have been reviewed. The nanosecond nonlinear absorption and the optical limiting abilities of these axially modified gallium phthalocyanines and naphthalocyanines in the optical region between the Q- and B-bands are shown to be dominated by a



**Scheme 3** Synthesis of fluorine-containing gallium naphthalocyanines **10,11**: (i)  $^n\text{BuLi}$ ,  $\text{Et}_2\text{O}$ ,  $-78^\circ\text{C}$ , 2 h; (ii) 1-methylpyrrole, r.t., 50%; (iii) 3,6-bis(2-pyridyl)-1,2,4,5-tetrazine, 83%; (iv) dicyanoacetylene,  $\text{CHCl}_3$ ,  $0^\circ\text{C}$ ; (v) 3-chloroperoxybenzoic acid, r.t., 67%; (vi)  $\text{GaCl}_3$ ,  $200^\circ\text{C}$ , 30 min, 36%; (vii) conc.  $\text{H}_2\text{SO}_4$ ,  $-10$  to  $-20^\circ\text{C}$ , 2 h, 46%.

strong triplet excited state absorption. The spectral bandwidth or window over which the limiter operates, and the ground-state and excited-state spectra and lifetimes, can be engineered by altering the axial or peripheral substituents, central metal cations and the structure of the main rings. From the practical

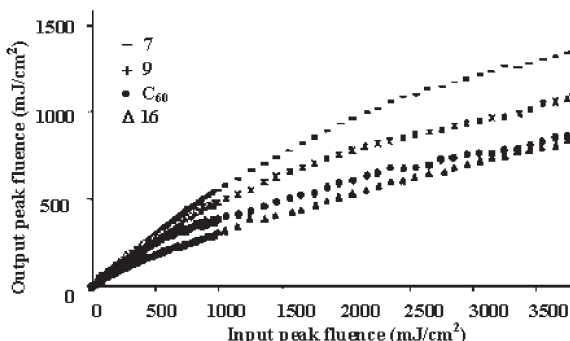


**Fig. 11** Comparison of the optical limiting performance for  $\text{C}_{60}$ , **7**, **9**, and **16** under the same measurement condition.

limiting application point of view, the better nonlinear optical materials required for practical optical devices must meet the following four standards: (1) highly soluble compounds with weaker intermolecular interaction; (2) a high linear transmission; (3) a large nonlinear absorption with a sub-nanosecond response time over a broad spectral bandwidth; and (4) a high threshold for damage. Meeting all these criteria is still a significant chemical challenge.

Further improvements in the limiting properties of metallophthalocyanines could be realized by a small increase in the ground state cross section near the minimum absorbance. This would give a larger nonlinear absorption coefficient and a smaller threshold in this region. It could be achieved either by a change in molecular structure or by introducing a second absorber in this range, provided the absorber effectively transferred the excitation energy to the phthalocyanine.<sup>12</sup> It may also be possible to manipulate the molecular structure at the axial position to give the material desirable physical properties without large changes in the optical properties. By linking an optically active chromophore as an axial ligand,  $\text{Pc}$ 's with axial chirality can be prepared.<sup>46</sup> Dimetallic binuclear phthalocyanines may be designed and synthesized for optical limiting purposes. In this case, a cooperative effect between the two halves of the molecules is expected. Based on past theoretical studies of organic materials which exhibit noted nonlinear absorption an in depth study into the resulting properties for solution and solid state based system (by polymerizing the suitably substituted phthalocyanines<sup>47</sup> or, embedding the phthalocyanines as inclusions in a polymer host to form a composite material<sup>48</sup>), and a detailed understanding of the factors affecting the NLO and OL response would be among major ongoing areas of effort.

## Acknowledgements

The authors would particularly like to express their thanks to Prof. W. J. Blau and Dr. S. M. O'Flaherty of the Physical Department at Trinity College Dublin (Ireland) for the NLO and OL measurements. We are grateful for the financial support of Deutsche Forschungsgemeinschaft (Projekt Ha 280/165-1), National Natural Science Foundation of China, East China University of Science and Technology, and China/Ireland Science and Technology Collaboration Research Foundation, respectively. Y. Chen also thanks the Alexander von Humboldt Foundation of Germany and Japan Science and Technology Agency for a fellowship.

**Yu Chen,\*<sup>abc</sup> Michael Hanack,<sup>b</sup> Yasuyuki Araki<sup>c</sup> and Osamu Ito<sup>c</sup>**

<sup>a</sup>Department of Chemistry, Lab for Advanced Materials, East China University of Science and Technology, 130 Melling Road, Shanghai 200237, People's Republic of China. E-mail: chentangyu@yahoo.com

<sup>b</sup>Institut für Organische Chemie, Organische Chemie II, Universität Tübingen, Auf der Morgenstelle 18, 72076 Tübingen, Germany

<sup>c</sup>Institute of Multidisciplinary Research for Advanced Materials, CREST(JST), Tohoku University, Katahira2-1-1, Sendai 980-8577, Japan

## References

- 1 H. S. Nalwa and J. S. Shirk, in *Phthalocyanines: Properties and Applications*, Eds. C. C. Leznoff, A. B. P. Lever, VCH Publishers, Inc., New York, 1996, vol. 4, p. 83.

2 M. Hanack and M. Lang, *Adv. Mater.*, 1994, **6**, 819.

3 N. B. McKeown, *Phthalocyanine Materials: Synthesis, Structure and Function*, Eds. B. Dunn, J. W. Goodby and A. R. West, Cambridge University Press, 1998.

4 (a) G. De La Torre, P. Vazquez, F. Agullo-Lopez and T. Torres, *J. Mater. Chem.*, 1998, **8**, 1671; (b) G. De La Torre, P. Vazquez, F. Agullo-Lopez and T. Torres, *Chem. Rev.*, 2004, **104**, 3723.

5 N. Kobayashi, N. Sasaki, Y. Higashi and T. Osa, *Inorg. Chem.*, 1995, **34**, 1636.

6 G. Schmid, E. Witke, U. Schlick, S. Knecht and M. Hanack, *J. Mater. Chem.*, 1995, **5**, 855.

7 (a) S. O'Flaherty, S. V. Hold, M. J. Cook, T. Torres, Y. Chen, M. Hanack and W. J. Blau, *Adv. Mater.*, 2003, **15**, 19; (b) M. Calvete, G. Y. Yang and M. Hanack, *Synth. Met.*, 2004, **141**, 231.

8 Z. Z. Ho, C. Y. Ju and W. M. Hetherington, III., *J. Appl. Phys.*, 1987, **62**, 716.

9 H. Matsuda, S. Okada, A. Masaki, H. Nakanishi, Y. Suda, K. Shigehara and A. Yamada, *SPIE Proc.*, 1990, **1337**, 105.

10 Y. Chen, D. Dini, M. Hanack, M. Fujitsuka and O. Ito, *Chem. Commun.*, 2004, 340.

11 D. R. Coulter, V. M. Miskowski, J. W. Perry, T. H. Wei, E. W. Van Stryland and D. J. Hagan, *SPIE Proc.*, 1989, **1105**, 42.

12 (a) J. S. Shirk, R. G. S. Pong, S. R. Flom, H. Heckmann and M. Hanack, *J. Phys. Chem. A*, 2000, **104**, 1438; (b) H. Heckmann, *Ph.D Thesis*, University of Tübingen, Germany, 1999.

13 M. Sanghadasa, I. S. Shin, R. D. Clark, H. Guo and B. G. Penn, *J. Appl. Phys.*, 2001, **90**, 31.

14 L. W. Tutt and T. F. Boggess, *Prog. Quantum Electron.*, 1993, **17**, 299.

15 M. Pittman, P. Plaza, M. M. Martin and Y. H. Meyer, *Opt. Commun.*, 1998, **158**, 201.

16 P. L. Chen, I. V. Tomov, A. S. Dvornikov, M. Nakashima, J. F. Roach, D. M. Alabran and P. M. Rentzepis, *J. Phys. Chem.*, 1996, **100**, 17507.

17 C. W. Spangler, *J. Mater. Chem.*, 1999, **9**, 2013.

18 W. Su and T. M. Cooper, *Chem. Mater.*, 1998, **10**, 1212.

19 T. Xia, A. Dogatiu, K. Mansour, D. J. Hagan and A. A. Said, *J. Opt. Soc. Am. B*, 1998, **15**, 1497.

20 L. Smilowitz, D. McBranch, V. Klimov, J. M. Robinson, A. Koskelo, M. Grigorova, B. R. Mattes, R. C. H. Wang and F. Wudl, *Opt. Lett.*, 1996, **21**, 922.

21 (a) A. Krivokapic, H. L. Anderson, G. Bourhill, R. Ives, S. Clark and L. J. McEwan, *Adv. Mater.*, 2001, **13**, 652; (b) G. Brusatin and R. Signorini, *J. Mater. Chem.*, 2002, **12**, 1964.

22 S. R. Flom, J. S. Shirk, R. G. S. Pong, F. J. Bartoli, A. W. Snow and M. E. Boyle, *Abstr. Pap.-Am. Chem. Soc.*, 1996, **212th**, PMSE-124.

23 B. H. Cumpston, K. Mansour, A. A. Heikal and J. W. Perry, *Mater. Res. Soc. Symp. Proc.*, 1997, **479**, 89.

24 (a) M. Sheik-Bahae, A. A. Said, T. H. Wie, D. J. Hagan and E. W. Van Stryland, *IEEE J. Quantum Electron.*, 1990, **26**, 760; C. H. Kwak, Y. L. Lee and S. G. Kim, *J. Opt. Soc. Am. B*, 1999, **16**, 600.

25 Y. Chen, L. R. Subramanian, M. Barthel and M. Hanack, *Eur. J. Inorg. Chem.*, 2002, 1032.

26 Y. Chen, M. Fujitsuka, S. M. O'Flaherty, M. Hanack, O. Ito and W. J. Blau, *Adv. Mater.*, 2003, **15**, 899.

27 Y. Chen, S. M. O'Flaherty, M. Hanack and W. J. Blau, *J. Mater. Chem.*, 2003, **13**, 2405.

28 Y. Chen, L. R. Subramanian, M. Fujitsuka, O. Ito, S. O'Flaherty, W. J. Blau, T. Schneider, D. Dini and M. Hanack, *Chem. Eur. J.*, 2002, **8**, 4248.

29 V. Krishnan, M. P. Feth, E. Wendel, Y. Chen, M. Hanack and H. Bertagnolli, *Z. Phys. Chem.*, 2004, **218**, 1.

30 C. G. Claessens, A. Gouloumis, M. Barthel, Y. Chen, G. Martin, F. Agullo-Lopez, I. Ledoux-Rak, J. Zyss, M. Hanack and T. Torres, *J. Porphyrins Phthalocyanines*, 2003, **7**, 291.

31 (a) M. Gouterman, G. H. Wagniere and L. C. Synder, *J. Mol. Spectrosc.*, 1963, **11**, 108; (b) A. J. McHugh and M. Gouterman, *Theor. Chim. Acta*, 1972, **24**, 346; (c) C. Weiss, H. Kobayashi and M. Gouterman, *J. Mol. Spectrosc.*, 1965, **16**, 415.

32 Y. Chen, Y. Araki, M. Fujitsuka, M. Hanack, O. Ito, S. M. O'Flaherty and W. J. Blau, *Solid State Commun.*, 2004, **131**, 773.

33 W. Uhl, T. Spies and R. Koch, *J. Chem. Soc., Dalton Trans.*, 1999, 2385.

34 P. Wei, X. W. Li and G. H. Robinson, *Chem. Commun.*, 1999, 1287.

35 K. S. Klimek, C. Cui, H. W. Roesky, M. Noltemeyer and H. G. Schmidt, *Organometallics*, 2000, **19**, 3085.

36 W. Uhl and T. Spies, *Z. Anorg. Allg. Chem.*, 2000, **626**, 1059.

37 H. Bertagnolli, W. J. Blau, Y. Chen, D. Dini, M. P. Feth, S. M. O'Flaherty, M. Hanack and V. Krishnan, *J. Mater. Chem.*, 2005, **15**, 683-689.

38 K. J. Wynne, *Inorg. Chem.*, 1984, **23**, 4658.

39 Y. Chen, M. Barthel, M. Seiler, L. R. Subramanian, H. Bertagnolli and M. Hanack, *Angew. Chem. Int. Ed.*, 2002, **41**, 3239.

40 H. S. Nalwa, A. Kakuta and A. Mukoh, *J. Phys. Chem.*, 1993, **97**, 1097.

41 H. S. Nalwa, M. Hanack, G. Pawlowski and M. K. Engel, *Chem. Phys.*, 1999, **245**, 17.

42 W. E. Ford, M. A. J. Rodgers, L. A. Schechtman, J. R. Sounik, B. D. Rihter and M. E. Kenney, *Inorg. Chem.*, 1992, **31**, 3371.

43 Y. Chen, S. O'Flaherty, M. Fujitsuka, M. Hanack, L. R. Subramanian, O. Ito and W. J. Blau, *Chem. Mater.*, 2002, **14**, 5163.

44 D. Dini, G. Y. Yang and M. Hanack, *J. Chem. Phys.*, 2003, **119**, 4857.

45 G. Y. Yang, M. Hanack, Y. W. Lee, Y. Chen, M. K. Y. Lee and D. Dini, *Chem. Eur. J.*, 2003, **9**, 2758.

46 N. Kobayashi, *Coord. Chem. Rev.*, 2001, **219-221**, 99.

47 Y. Chen, M. Hanack, S. M. O'Flaherty, G. Bernd, A. Zeug, B. Roeder and W. J. Blau, *Macromolecules*, 2003, **36**, 3786.

48 J. J. Doyle, S. M. O'Flaherty, Y. Chen, T. Hegarty, M. Hanack and W. J. Blau, *Proc. SPIE-Photonics Eur.*, 2004, **5464**, 269.